Available online at www.sciencedirect.com
ScienceDirect
Journal of Chromatography B, 853 (2007) 38–46
JOURNAL OF CHROMATOGRAPHY B
www.elsevier.com/locate/chromb

The suitability of DEAE-Cl active groups on customized poly(GMA-*co*-EDMA) continuous stationary phase for fast enzyme-free isolation of plasmid DNA

Michael K. Danquah, Gareth M. Forde *

BEL (Bio Engineering Laboratory), Department of Chemical Engineering, Monash University, Wellington Road, Melbourne 3800, Australia

Received 29 January 2007; accepted 23 February 2007
Available online 14 March 2007

Abstract

The creation of a commercially viable and a large-scale purification process for plasmid DNA (pDNA) production requires a whole-systems continuous or semi-continuous purification strategy employing optimised stationary adsorption phase(s) without the use of expensive and toxic chemicals, avian/bovine-derived enzymes and several built-in unit processes, thus affecting overall plasmid recovery, processing time and economics. Continuous stationary phases are known to offer fast separation due to their large pore diameter making large molecule pDNA easily accessible with limited mass transfer resistance even at high flow rates. A monolithic stationary sorbent was synthesised via free radical liquid porogenic polymerisation of ethylene glycol dimethacrylate (EDMA) and glycidyl methacrylate (GMA) with surface and pore characteristics tailored specifically for plasmid binding, retention and elution. The polymer was functionalised with an amine active group for anion-exchange purification of pDNA from cleared lysate obtained from *E. coli* DH5α-pUC19 pellets in RNase/protease-free process. Characterization of the resin showed a unique porous material with 70% of the pores sizes above 300 nm. The final product isolated from anion-exchange purification in only 5 min was pure and homogenous supercoiled pDNA with no gDNA, RNA and protein contamination as confirmed with DNA electrophoresis, restriction analysis and SDS page. The resin showed a maximum binding capacity of 15.2 mg/mL and this capacity persisted after several applications of the resin. This technique is cGMP compatible and commercially viable for rapid isolation of pDNA.

Keywords: Plasmid DNA; Methacrylate monolith; Fast purification; Enzyme-free process

1. Introduction

Orthodox particulate stationary phases for chromatographic separation are prepared by packing micrometer sized porous particles into a column. Separation of biomolecules occurs in the pores of the particles; therefore, the rate of separation is diffusion limited, hence the rate can be increased only at the expense of lower separation quality. The purification of large biomolecules, such as pDNA is weighed-down by the performance of conventional chromatographic supports with a small particle pore diameter. Most of these chromatographic supports are geared towards high adsorption capacity of proteins with size less than 5 nm [1]. In columns packed with such supports, pDNA with size greater than 100 nm adsorb predominantly on the outer surface of the particles. Consequently binding capacities are in the order of tenths of mg pDNA/mL support compared to 200 mg/mL reported for proteins [2]. Also Ghose et al., 2003 [3] observed from confocal microscopy that about 81% of the internal surface area of a conventional support with pore diameter 80 nm was unutilised after its application for plasmid purification. Relatively low flow rates together with low capacity result in low productivities and low time yields.

Continuous stationary phases are essential tools for bioseparation and biotransformation, thereby establishing position in biotechnology as adsorbent for the purification of biomolecules. These materials are characterised by low mass transfer resistance. Thus, all applications involving large molecules exhibit in principle better performance compared to conventional beaded media. A monolith is a continuous phase consisting of a piece of highly porous organic or inorganic solid material. The most essential feature of this support is that all the mobile phase is forced to flow through its large pores [4]. As a consequence, mass transport is steered by convection;

* Corresponding author.

1570-0232/$ – see front matter © 2007 Elsevier B.V. All rights reserved.
doi:10.1016/j.jchromb.2007.02.050

reducing the long diffusion time required by particle-based supports. Chromatographic separation process on monoliths is therefore virtually not diffusion-limited. The large pores of these monoliths allow penetration of pDNA molecules to the internal surface area; facilitating the accessibility of pDNA molecules by the internal active sites of the resin and minimizing pressure drop [5]. There exists generally a trade-off between pressure drop and binding capacity as increasing pore size decreases binding capacity (decreasing surface area) and decreasing pore size increases pressure drop. Different types of monolithic supports currently available are cryogels from polyacrylamide [6,7], emulsion-derived monoliths [8], polymethacrylate based polymers synthesised by free radical polymerisation induced thermally [8–13] or by radiation [14], silica columns manufactured as single blocks by a sol–gel process [15,16], silica xerogels [17], monoliths prepared from compressed polyacrylamide gels [18,19], polymer monoliths prepared through metathesis [20], monoliths prepared from carbon microspheres [21,22], carbon monoliths [21], cellulose-based monoliths [23], superporous agarose gel [24], poly vinyl alcohol [25], polyacrylamide-coated ceramics [26] and rolled woven fabrics [27]. Polymethacrylate monolithic supports are optimal adsorbents for pDNA separation. These adsorbents can be engineered to have large pore diameters thus no significant impedance to convective mass transport is expected. They can easily be modified by functionalising with an anion-exchange, hydrophobic interaction or affinity ligand depending on the type of purification technique to be employed. They are resistant to pH, non-toxic and economically favourable to synthesize. The flexibility and the ease to tailor their pore and surface characteristics to the target pDNA molecule through alteration in synthesis conditions makes them more attractive. This present study explores the synthesis and characterization of customized poly(GMA-*co*-EDMA) matrix with surface and pore distribution tailored distinctively for pDNA binding, retention and elution. The prospect of 2-chloro-*N*,*N*-diethylethylamine hydrochloride (DEAE-Cl) activated methacrylate monolith for single-stage fast anion exchange pDNA purification was investigated. The effect of ionic strength of the mobile phase on the plasmid size in relation to the co-purification of contaminants is also considered. Mathematical evaluation of the pressure drop across the methacrylate monolithic bed employing nodal analysis is presented.

2. Materials and methods

2.1. Materials

EDMA (M_w 198.22, 98%), GMA (M_w 142.15, 97%), cyclohexanol (M_w 100.16, 99%), 1-dodecanol (M_w 186.33, 98%), AIBN (M_w 164.21, 98%), MeOH (HPLC grade, M_w 32.04, 99.93%), DEAE-Cl (M_w 172.10, 97%) were purchased from Sigma–Aldrich. NaCl (Amresco, M_W 58.44, 99.5%), agarose (Promega), SDS (Amresco, M_w 288.38, 99.0%), Na_2CO_3 (SPECTRUM, M_w 105.99, 99.5%), Tris (Amresco, M_w 121.14, 99.8%), EDTA (SERVA, M_w 292.3, AG), EtBr (Sigma, M_w 394.31, 10 mg/mL), 1 kbp DNA marker (BioLabs, New England), Wizard plus SV Maxipreps (Promega).

2.2. Methods

2.2.1. Synthesis of methacrylate monolith and DEAE-Cl functionalisation of the epoxy groups

The methacrylate monolith was prepared via free radical liquid porogenic co-polymerisation of EDMA as the crosslinker and GMA as the functional monomer. EDMA/GMA mixture was combined with an alcohol-based bi-porogen solvent in the proportion 20/20/50/10 (GMA/EDMA/cyclohexanol/1-dodecanol) making a solution with total volume 10 mL. AIBN (1% weight with respect to monomer) was used to initiate the polymerisation process. The polymer mixture was sonicated for 10 min and sparged with N_2 gas to expel dissolved O_2. 5 mL of the mixture was gently transferred into a 12 cm × 1.5 cm polypropylene column (BIORAD) sealed at the bottom end. The top end was sealed with a rubber bung and placed in a water bath for 18 h at 50 °C. The remaining was polymerised under similar condition in a similar column for characterization. The polymer resin was washed to remove all porogens and other soluble matters with methanol in a soxhlet extractor for 20 h and dried at 70 °C. The polymer was washed with 0.5 M Na_2CO_3, 1.0 M NaCl, pH 11.5 followed by 50 g/L solution of DEAE-Cl and the reaction was allowed to proceed for 15 h at 60 °C. The resulting resin was washed with DI water for 30 min and dried at 70 °C. The ligand density was found to be 1.85 mmol DEAE-Cl/g resin according to the procedure outlined by Lindero et al., 2005 [28]. Reaction schemes for the synthesis and DEAE-Cl functionalisation of the poly(GMA-*co*-EDMA) monolith are shown in Fig. 1.

2.2.2. Preparation of clarified lysate from concentrated cell paste

Concentrated frozen cells of *E. coli* DH5α-pUC19 were thawn and resuspended by adding 50 mL of 0.05 M Tris–HCl, 0.01 M EDTA, pH 8 buffer to 5 g of bacterial cell paste and vortexing till a uniform suspension was obtained. The resuspended cells were contacted and homogenously mixed with the same volume of lysis solution (0.2 M NaOH, 1% SDS) for 3 min. Neutralization was performed by the addition of an equal volume of 3 M CH_3COOK at pH 5.5 to the lysed cell suspension. This neutralisation step causes renaturation of pDNA through its persistent anchor base pairs under the set pH condition. After gently mixing for 2 min, the mixture of pDNA-containing lysate and the precipitated impurities, mainly gDNA were separated to obtain a clarified lysate. This clarification step was conducted by centrifugation at 4600 × *g* for 20 min. The resulting clarified alkaline lysate typically contains pDNA, proteins, RNA, trace fragments of gDNA and lipopolysaccharides.

2.2.3. Standard plasmid preparation: maxiprep

Standard pDNA purification from the bacterial cell was performed with Wizard plus SV Maxipreps according to the manufacturer's instructions (Promega).

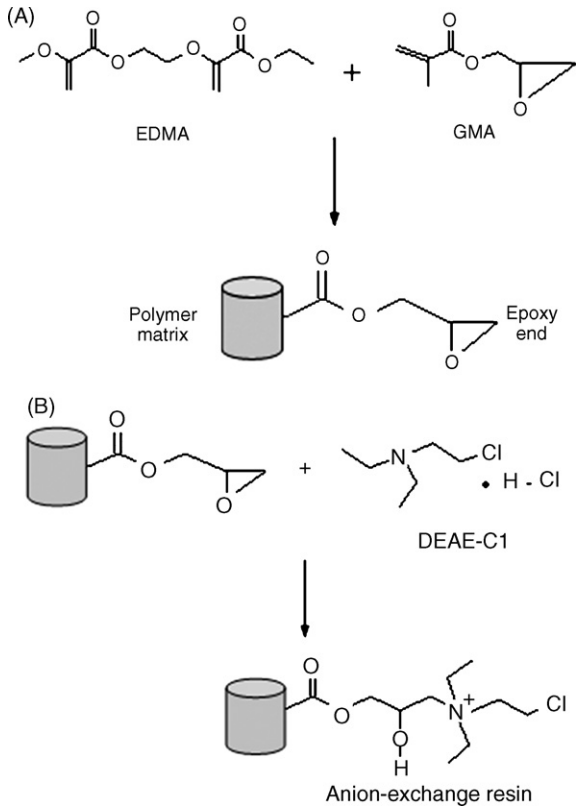

Fig. 1. (A) Polymerisation reaction between ethylene glycol dimethacrylate (EDMA) and glycidyl methacrylate (GMA). Reaction was carried out with cyclohexanol/dodecanol porogen at 50 °C for 18 h. (B) Reaction of 2-chloro-*N*,*N*-diethylethylamine hydrochloride functionalisation of epoxy groups on EDMA/GMA polymer. Reaction was carried out at 60 °C for 15 h.

2.2.4. Characterisation of polymer resin

The monolith inside the column was pushed out carefully, dried at 70 °C for 15 h and cut into disc-size pieces with a blade. The porous properties in the dry state were studied by Hg intrusion porosimetry, using a micrometrics Hg porosimeter (Autopore III, USA). The specific surface area of the resin was determined using Micromeritics ASAP 2020 instrument, USA via nitrogen adsorption/desorption isotherm. A piece of the monolith was placed on a sticky carbon foil that was attached to a standard aluminium specimen stub. The sample was vapour deposited with gold using a sputter coater (Dynavac, model SC 150, Australia). Microscopic analysis of the sample was carried out using a high resolution field emission scanning electron microscope (JEOL JSM-6300F, Japan) at a voltage of 15 kV.

2.2.5. Anion-exchange purification of pDNA

BIORAD polypropylene column 12 cm × 1.5 cm containing 5 mL of DEAE-Cl functionalised monolithic resin was connected with a movable adaptor and configured to BIORAD HPLC system. Chromatographic purification of pDNA was performed using 25 mM Tris–HCl, 2 mM EDTA, 0.2 M NaCl, pH 8.1 as buffer A and 25 mM Tris–HCl, 2 mM EDTA, 1.0 M NaCl, pH 8.1 as buffer B. Prior to the purification experiment, the column was equilibrated with 3 CV of buffer A. To reconnoitre a proper chromatographic condition, 20 μL of sample of the clarified lysate was diluted (×0.5) with buffer A and applied at 1 mL/min. After washing the unbound and weakly retained molecules with buffer A, the ionic strength of buffer A was linearly and stepwisely increased by mixing proportionally buffer A with buffer B and bound species were eluted.

2.2.6. Quality and purity of pDNA samples

The purity and concentration of pDNA samples were determined spectrophometrically at 260 nm and 280 nm. Optical density of 1.0 measured at 260 nm with light path of 1 cm represent 50 mg dsDNA/L. Absorption measurements taken at wavelengths of 260 nm and 280 nm were used to determine the purity of pDNA based on the ratio OD260/OD280 which is expected to be within 1.7–1.9 to indicate the sample is free of protein contamination. Nature and size of pDNA were determined by EtBr agarose gel electrophoresis using a 1 kbp DNA ladder. Gel was made up in ×50 dilution of TAE buffer (242 g of Tris base, 57.1 mL CH_3COOH, 9.305 g of EDTA), stained with 3 μg/mL EtBr and run at 66 V for 2 h. The resulting fractionated nucleic acid gel is visualised and photographed (BIORAD, Universal Hood II, Italy).

2.2.7. Column sanitation and regeneration procedure

Column cleaning was performed by washing the column with 400 CVs of a solution containing 0.5 M NaOH, 2 M NaCl and 10% EtOH followed by another 400 CVs of only 10% EtOH solution. The column is then regenerated with 400 CVs of 25 mM Tris–HCl, 2.0 M NaCl, pH 8.1 and equilibration was performed with the appropriate starting buffer until a constant UV baseline was obtained.

3. Results

3.1. Dependency of pDNA size on ionic strength of binding buffer

The sizes of standard pDNA samples under different conditions of ionic strength of binding buffer were determined using a mastersizer (Malvern 2000, Australia). The ionic strength of the binding buffer was increased by increasing sodium chloride concentration thus increasing $[Na^+]$ in solution. Plasmid DNA stock solution in TE buffer (25 mM Tris–HCl, 2 mM EDTA, pH 8.1) was analysed for conformational changes under different ionic strength of the binding buffer. The average *D*[4,3] readings for 5 runs of pDNA samples are 126 nm, 190 nm and 207 nm in the buffer with NaCl concentrations of 1.0 M, 0.5 M and 0 M, respectively (Fig. 2; Table 1). The data obtained revealed that at low ionic strength, pDNA molecules are loosely interwound supercoils, while plectonemic superhelices are formed in higher ionic concentration. Plasmid DNA is a highly charged polymer, so the electrostatic repulsion of negatively charged pDNA helices opposes folding and formation of close contacts between charged regions. However, counterions shield the negative charge of pDNA and hence decrease the repulsion between charged segments. Consequently, the geometry of supercoiled pDNA changed at different ionic conditions. High concentration

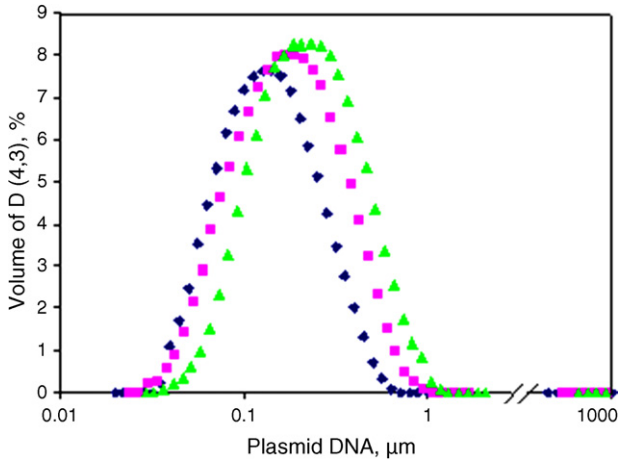

Fig. 2. Dependency of plasmid size on ionic strength of binding buffer. Ionic strength of the binding was increased by increasing concentration of NaCl from 0 M → 0.5 M → 1.0 M. The D[4,3] values obtained are 207 nm, 190 nm and 126 nm for 0 M, 0.5 M and 1.0 M, respectively. (▲) 0 M NaCl, (■) 0.5 M NaCl and (♦) 1.0 M NaCl.

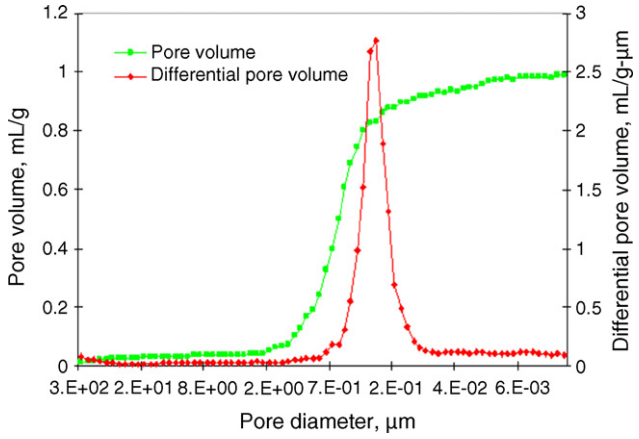

Fig. 3. Cumulative pore volume and differential pore volume against pore diameter of the monolith composed of 20/20/50/10 GMA/EDMA/cyclohexanol/1-dodecanol using mercury intrusion porosimeter. The plot shows a modal pore diameter of 300 nm existing in the matrix and a total pore volume of 0.95 mL/g.

of metal ions in the pDNA solution resulted in the shrinking of the pDNA molecules; thus reducing plasmid size.

3.2. Characterization and performance of methacrylate monolithic resin

3.2.1. Porosimetry and surface characterization

Pores analysis of the resin showed a unimodal pore size distribution with a maximum occurring pore diameter of 300 nm. This value shows a suitable pore diameter for use as a stationary phase for pDNA binding and retention considering the plasmid size under the binding buffer conditions. The total pore volume obtained is 0.95 mL/g and this value represents a good holding and retention capacity of the monolith (Fig. 3). About 70% of the pores within the matrix have diameters greater than 300 nm. The BET surface area of 15.7 m^2/g obtained from nitrogen adsorption–desorption isotherm at 77 K shows the existence of relatively few mesopores within the matrix in comparison with macropores. SEM reveals porous network structure of the polymer matrix. Picture shows large pores existing within the matrix giving a pictorial confirmation of the pore behaviour obtained (Fig. 4).

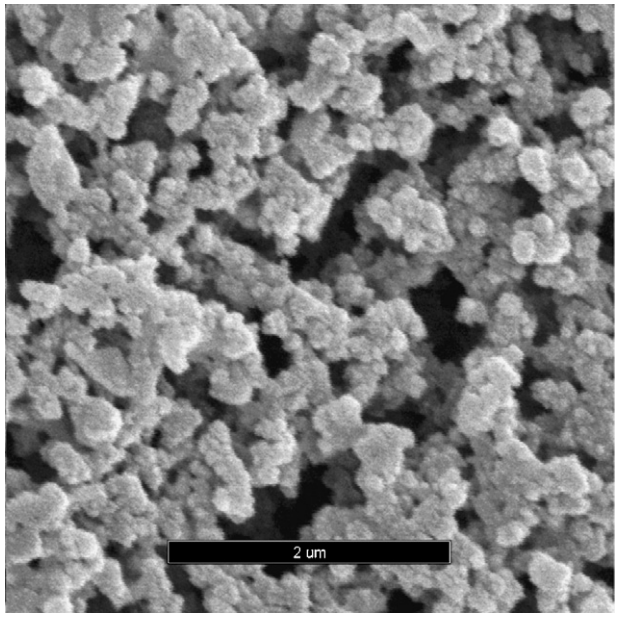

Fig. 4. SEM picture for the monolith composed of 20/20/50/10 GMA/EDMA/cyclohexanol/1-dodecanol. The picture shows large throughpores of the monolith and the network structure of the polymerised feed stock. Picture was obtained at ×20,000 magnification and 15 kV operating voltage.

3.2.2. Analytical chromatography

Different concentrations of the plasmid standards were prepared using Wizard Plus SV Minipreps according to the manufacturer's instructions and 5 μL of each injected in the DEAE-Cl functionalised resin to create a calibration curve. Similar chromatographic features were obtained for the different

Table 1
Plasmid DNA size analysis in different ionic strength of binding buffers TE (25 mM Tris–HCl, 2 mM EDTA, pH 8.1)

pDNA sample	pDNA size $D_{[4.3]}$ (nm)	Resin Pore size (nm), ligand density (mmol/g)	ΔP_{avg} (MPa)	Binding capacity (mg/mL)	
				1 mL/min	3 mL/min
pUC19 + TE + 0 M NaCl	207	poly(GMA-*co*-EDMA) + DEAE-Cl, 300 nm, 1.85 mmol/g	45.8	12.10	11.12
pUC19 + TE + 0.5 M NaCl	190	poly(GMA-*co*-EDMA) + DEAE-Cl, 300 nm, 1.85 mmol/g	36.3	15.20	13.81
pUC19 + TE + 1.0 M NaCl	126	poly(GMA-*co*-EDMA) + DEAE-Cl, 300 nm, 1.85 mmol/g	19.1	10.32	8.94

Dynamic binding capacities were determined using poly(GMA-*co*-EDMA) + DEAE-Cl resin with pore size 300 nm and ligand density 1.85 mmol/g.

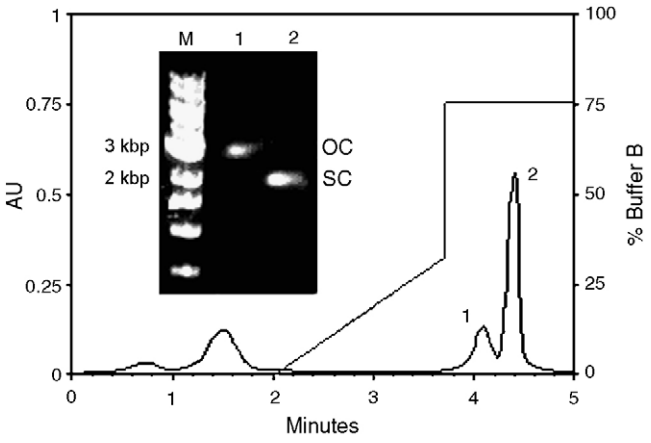

Fig. 5. Anion-exchange chromatography of pDNA obtained using Wizard plus SV Maxipreps kit. Stationary phase: DEAE-Cl functionalised methacrylate monolith with active group density 1.85 mmol DEAE-Cl/g resin and modal pore size 300 nm. Chromatographic conditions—Buffer A: 25 mM Tris–HCl, 2 mM EDTA, 0.2 M NaCl pH 8.1; Buffer B: 25 mM Tris–HCl, 2 mM EDTA, 1.0 M NaCl, pH 8.1; Sample: 5 μL of cleared cell lysate. Flow rate, 1 mL/min. Gradient elution, 0–0.325 M for 102 s and step elution, 0.325–0.75 M for 78 s. Peaks 1 and 2 represent open circular and supercoiled pDNA, respectively. Inset shows EtBr agarose gel electrophoresis of the pDNA fractions. Analysis was performed using 1% agarose in TAE × 1 buffer, 3 μg/ml EtBr at 66 V for 2 h. Lane M is 1 kbp DNA ladder; lanes 1 and 2 represent open circular and supercoiled pDNA, respectively.

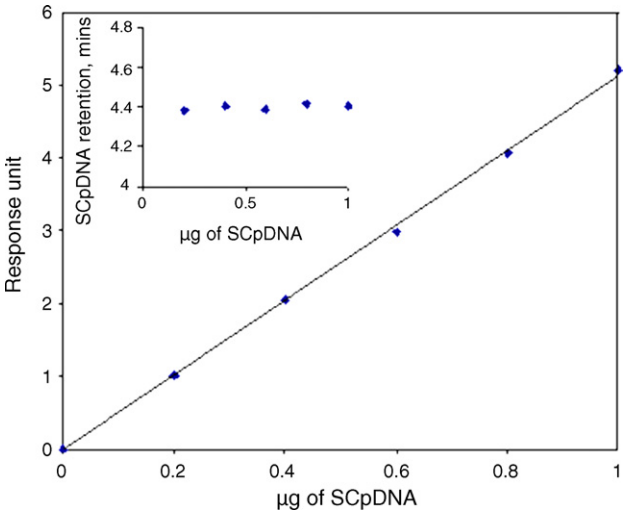

Fig. 6. Standard calibration curve for different concentration of supercoiled pDNA and the UV response units (1 RU = 5.16 μg of Sc pDNA). Plasmid samples were obtained from Wizard plus SV Maxiprep. Retention time was found to be independent of plasmid concentration according to the inset.

plasmid concentrations. A representative chromatogram for the plasmid samples is shown in Fig. 5. The similar characteristic features of the chromatograms are: a peak at 1.50 min which corresponds to 25 mM Tris–HCl, 2 mM EDTA, pH 8.1 buffer washing and peaks 1 and 2 showing the presence of open circular ($A_{260}/A_{280} = 1.84$) and supercoiled ($A_{260}/A_{280} = 1.89$) plasmid forms at 4.09 and 4.40 min average retention time, respectively. The retention time of the supercoiled plasmid was usually in the range 4.38–4.42 min. The DEAE-Cl functionalised resin was found to be very suitable in the quantification of total supercoiled pDNA. A five point calibration curve was generated for supercoiled plasmid quantity in 260 nm UV absorbance response units (Fig. 6).

3.2.3. Dynamic binding capacity analysis

The influence of different [Na^+] on dynamic binding capacity of the standard pDNA obtained from Wizard plus SV Maxipreps was studied using the DEAE-Cl functionalised methacrylate resin. As shown in Table 1, the dynamic binding capacity increased (from 12.10 mg/mL to 15.20 mg/mL at 1 mL/min and 11.12 mg/mL to 13.81 mg/mL at 3 mL/min) with increasing [Na^+] (from 0 M to 0.5 M); representing decreasing pDNA size (from 207 nm to 190 nm). This observation can be explained by the increasing accessibility of the pDNA molecules by the inner active surfaces of the resin, thereby increasing interaction and retention. The results commensurate with decreasing pressure drop as pDNA molecules are decreasing in size and are therefore unable to block the pores existing in the resin matrix. Observation of pDNA capacity increase was recently reported on the use of compacting agents [29]. Further increase in [Na^+] to 1.0 M decreased pDNA size to 126 nm as expected but gave a lower dynamic binding capacity of 10.32 mg/ml and 8.94 mg/ml at 1 mL/min and 3 mL/min, respectively. This conflicting result is ascribed to the low binding performance associated with high resin pores size to pDNA size ratio; most plasmid molecules pass through the resin unbounded, thus resulting in reduced contact time and binding capacity at a very low pressure drop.

3.2.4. Single-stage purification of pDNA from clarified lysate: preparative chromatography

Plasmid DNA, a polymer of deoxyribonucleotides is anionic (two negatively charged phosphate groups per one base pair) over a wide range of pH and can therefore be isolated using DEAE-Cl functionalised resin which is a positively charged matrix. Fig. 7 shows the resulting chromatogram for the direct capture of pDNA from the cleared lysate. The chromatogram shows co-purification of protein and RNA contaminants resulting from the electrostatic binding between the positively charged matrix and negatively charged RNA and protein molecules existing with the target pDNA molecules in the cleared lysate. Bound RNA, proteins and pDNA molecules were eluted, respectively, as peaks 3, 4 and 5. Peak elution of the molecules is in order of increasing anionic charge density, a property which is in turn a function of size and conformation for a specific molecule. Pure supercoiled pDNA fraction ($A_{260}/A_{280} = 1.87$) was collected from peak 5 as revealed by the inserted EtBr agarose gel electrophoresis picture. Endotoxins, mainly lipopolysaccharides contain exposed hydrophobic groups and are therefore unable to interact with the anion-exchange resin; hence form part of the flow-through.

3.3. Evaluation of pressure drop across the monolithic bed employing multi-nodal analysis

Comparative pressure drop estimation was carried out for different porous monolithic media. The pressure drop across a monolithic bed is dependent on the type of porous media,

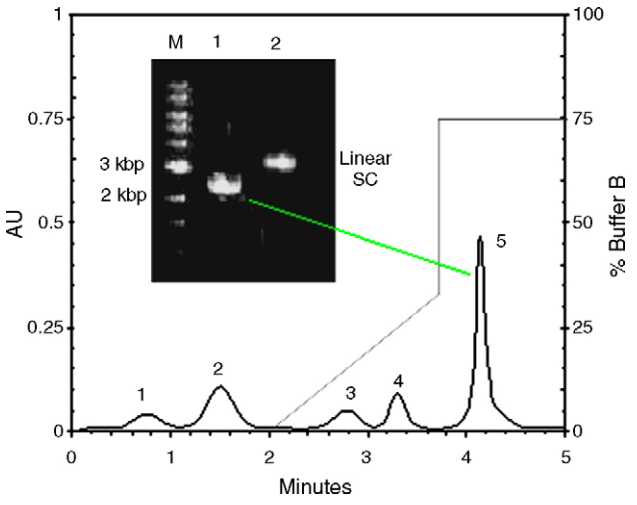

Fig. 7. Anion-exchange chromatographic purification of pDNA from *E. coli* DH5α-pUC19 cleared lysate using 5 mL DEAE-Cl functionalised methacrylate monolith with active group density 1.85 mmol DEAE-Cl/g resin and modal pore size 300 nm. Chromatographic conditions—Buffer A: 25 mM Tris–HCl, 2 mM EDTA, 0.2 M NaCl, pH 8.1; Buffer B: 25 mM Tris–HCl, 2 mM EDTA, 1.0 M NaCl, pH 8.1, flow rate; 1 mL/min. Peaks 1, 2, 3, 4 and 5 represent loading, washing, RNA, protein and pDNA, respectively. Inset shows results from EtBr agarose gel electrophoresis of pDNA fractions. Analysis was performed using 1% agarose in TAE × 1 buffer, 3 μg/mL EtBr at 66 V for 2 h. Lane M is 1 kbp DNA ladder; lanes 1 and 2 represent supercoiled pDNA and linear pDNA obtained from *Eco*RI cleavage at the sequence GAATTC of the supercoiled pDNA. Gel picture reveals no band for contaminants.

channel size and network structure. Two types of porous media are considered; the first (Fig. 8) is a monolithic structure made of homogeneous pores having equal diameters with channels not interconnected and the second (Fig. 9) is a monolithic structure with non-uniformity in pore structure with channels interconnected. Methacrylate monolithic resins synthesised via thermal free radical liquid porogenic copolymerisation of EDMA and GMA show pore structure similar to the latter. They have a

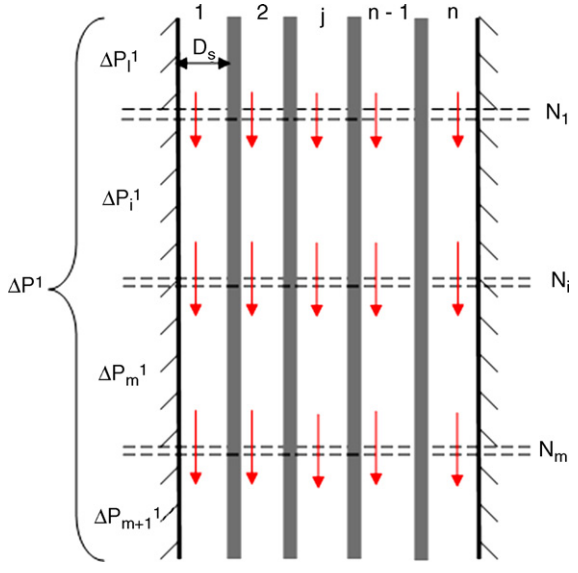

Fig. 8. A monolithic structure made of homogeneous pores having equal diameter with channels not interconnected.

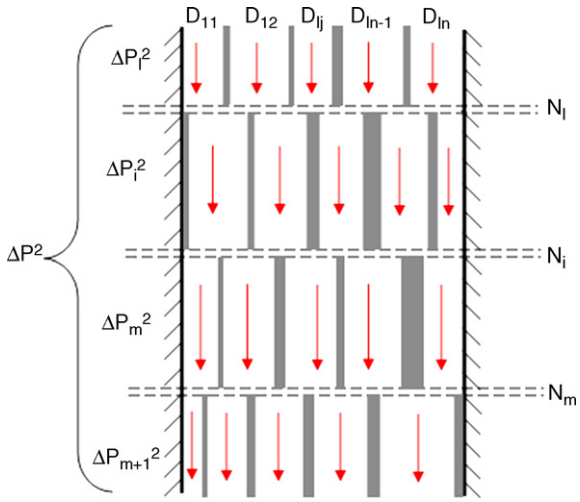

Fig. 9. A monolithic structure with non-uniformity in pore structure with channels interconnected.

combination of both identical and non-identical structure between nodes with pore interconnectivities. Hence, the entire porous structure is heterogeneous.

Let assume the same flow rate is applied to both structures, both structures have similar voidage with equal pore volume and that the pore volume existing in a nodal plane N_i is negligible. D_s is the pore diameter of the first porous media, D_j a pore diameter existing in the second porous media and ΔP_i^k ($k = 1, 2$) is the pressure drop across N_{i-1} and N_i nodal planes for porous media 1 and 2. Considering the first structure, pores of the same length have the same pore volume and since nodal planes are considered at the same intervals the pressure drop between successive nodal planes is the same. For m number of nodal planes,

$$\Delta P_1^1 = \Delta P_2^1 = \ldots = \Delta P_i^1 = \Delta P_{i+1}^1 = \ldots = \Delta P_m^1 = \Delta P_{m+1}^1 \quad (1)$$

Consequently, the total pressure drop ΔP^1 over the bed is given by;

$$\Delta P^1 = \Delta P_1^1 + \Delta P_2^1 + \cdots + \Delta P_i^1 + \Delta P_{i+1}^1 + \cdots + \Delta P_m^1 + \Delta P_{m+1}^1 = \sum_{i=1}^{i=m+1} \Delta P_i^1 = (m+1)\Delta P_i^1 \quad (2)$$

Total pore volume for a unit node to node interval, V_{p1} existing in pore media 1;

$$V_{p1} = n(m+1)\frac{\pi D_s^2}{4} \quad (3)$$

For the second structure, pore diameters between nodes are different so the pressure drops are different for any two consecutive nodal planes. Liquid flowing through this structure can randomly switch through the nodal planes from one pore to the other.

$$\Delta P_1^2 \neq \Delta P_2^2 \neq \ldots \neq \Delta P_i^2 \neq \Delta P_{i+1}^2 \neq \ldots \neq \Delta P_m^2 \neq \Delta P_{m+1}^2 \quad (4)$$

Consequently, the total pressure drop ΔP^2 over the bed is given by;

$$\Delta P^2 = \Delta P_1^2 + \Delta P_2^2 + \cdots + \Delta P_i^2 + \Delta P_{i+1}^2 + \cdots + \Delta P_m^2 + \Delta P_{m+1}^2 = \sum_{i=1}^{i=m+1} \Delta P_i^2 \quad (5)$$

Total flow-through in media 2 is equal to the sum of the individual flows in all the pores. D_{ij} represents the diameter of the jth pore entering the ith nodal plane. Total pore volume for a unit node to node interval, V_{p2} existing in pore media 2;

$$V_{p2} = \frac{\pi}{4}\left(\sum_{j=1}^{j=n} D_{1j}^2 + D_{2j}^2 + \cdots + D_{ij}^2 + \cdots + D_{mj}^2 + D_{(m+1)j}^2\right) = \frac{\pi}{4}\sum_{j=1}^{j=n}\sum_{i=1}^{i=m+1} D_{ij}^2 \quad (6)$$

Since the total pore volume for structures 1 and 2 are the same, $V_{p1} = V_{p2}$

$$n(m+1)\frac{\pi D_s^2}{4} = \frac{\pi}{4}\sum_{j=1}^{j=n}\sum_{i=1}^{i=m+1} D_{ij}^2 \Rightarrow n(m+1)D_s^2 = \sum_{j=1}^{j=n}\sum_{i=1}^{i=m+1} D_{ij}^2 \quad (7)$$

Pressure drop of a laminar flow through a cylindrical pore can be computed using the Hagen–Poiseuille equation. Application of Hagen–Poiseuille equation on structure 1 gives;

$$\phi_v^1 = n(m+1)\pi\frac{\Delta P^1 D_s^4}{128\eta L} \quad (8)$$

Application of Hagen–Poiseuille equation on structure 2 gives;

$$\phi_v^2 = \frac{\pi}{128\eta L}\sum_{j=1}^{j=n}\Delta P_{1j} D_{1j}^4 + \Delta P_{2j} D_{2j}^4 + \cdots + \Delta P_{ij} D_{ij}^4 + \cdots + \Delta P_{mj} D_{mj}^4 + \Delta P_{(m+1)j} D_{(m+1)j}^4 = \frac{\pi}{128\eta L}\sum_{j=1}^{j=n}\sum_{i=1}^{i=m+1}\Delta P_{ij} D_{ij}^4$$

Since the total pore volume existing in structures 1 and 2 are considered the same, $\phi_v^1 = \phi_v^2$

$$n(m+1)\pi\frac{\Delta P^1 D_s^4}{128\eta L} = \frac{\pi}{128\eta L}\sum_{j=1}^{j=n}\sum_{i=1}^{i=m+1}\Delta P_{ij} D_{ij}^4$$

$$\Rightarrow n(m+1)D_s^4\,\Delta P^1 = \sum_{j=1}^{j=n}\sum_{i=1}^{i=m+1}\Delta P_{ij} D_{ij}^4 \quad (9)$$

Combining Eqs. (7) and (9) gives;

$$\frac{\sum_{j=1}^{j=n}\sum_{i=1}^{i=m+1}(\Delta P_{ij}/\Delta P^1) D_{ij}^4}{D_s^2\sum_{j=1}^{j=n}\sum_{i=1}^{i=m+1} D_{ij}^2} = 1 \quad (10)$$

Considering a single nodal plane ($i=1$) of a non-uniform methacrylate monolithic structure which is bimodal ($j=2$) with modal pore diameters D_1 and D_2 in the ratio $D_1/D_2 = \xi$. Assume the monolith has a structure of parallel type non-uniformity. The pressure drop analysis for this system is carried out in comparison with a monolith of uniform structure having the same pore volume, single node ($i=1$) and unimodal pore diameter D_0.

Pore volume equality for the two systems can be written as;

$$D_0^2 = \frac{D_1^2}{2} + \frac{D_2^2}{2} = \frac{D_1^2}{2}\left(1 + \frac{D_2^2}{D_1^2}\right) = \frac{D_1^2}{2}\left(1 + \frac{1}{\xi^2}\right) \quad (11)$$

Applying Hagen–Poiseuille equation to evaluate pressure drop and equalising results gives;

$$2\,\Delta P_0 D_0^4 = \Delta P_1 D_1^4 + \Delta P_2 D_2^4 \quad (12)$$

For parallel type non-uniform structure, the total pressure drop above (ΔP_1) and below (ΔP_2) the nodal plane are the same; hence $\Delta P_1 = \Delta P_2 = \Delta P$

$$2\,\Delta P_0 D_0^4 = \Delta P(D_1^4 + D_2^4) = \Delta P D_1^4\left(1 + \frac{D_2^4}{D_1^4}\right) = \Delta P D_1^4\left(1 + \frac{1}{\xi^4}\right) \quad (13)$$

Combining Eqs. (11) and (13) gives;

$$\frac{\Delta P_0}{\Delta P} = 2\left(1 + \frac{1}{\xi^4}\right)\left(1 + \frac{1}{\xi^2}\right)^{-2} \quad (14)$$

Differentiating Eq. (14) gives;

$$\frac{\mathrm{d}(\Delta P_0/\Delta P)}{\mathrm{d}\xi} = \frac{8\xi}{(\xi^2+1)^2}\left(\xi^2 - \frac{\xi^4+1}{\xi^2+1}\right) \quad (15)$$

The minimum value of $(\Delta P_0/\Delta P)$ occurs at $\xi = 1$

The dependency of pressure drop on media type is shown in Fig. 10 for the single node structure with parallel type non-uniformity. It is obvious that for $0 < \xi < 1$ the parallel type non-uniform structure gives a higher pressure drop in comparison to the structure with uniform pore size distribution. For $\xi \geq 1$, the parallel type non-uniform structure gives a lower pressure drop in comparison to the structure with uniform pore size distribution. The profile obtained shows that low pressure drop can be obtained simply by modifying the pore size distribution. For methacrylate monolith, this can be achieved by altering synthesis conditions, such as polymerisation temperature, reactant mixture composition and heat transfer coefficients.

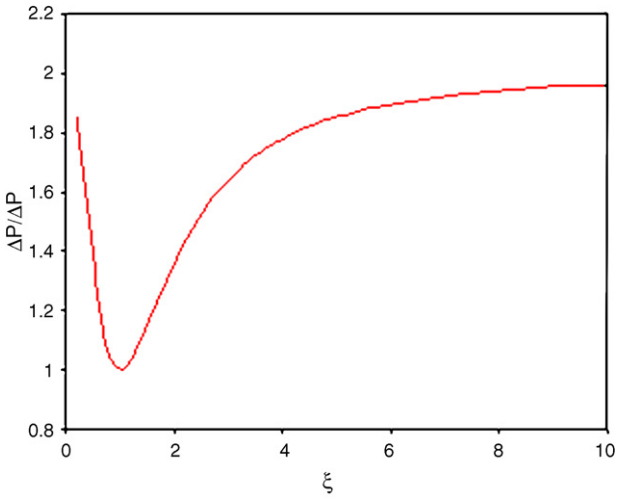

Fig. 10. Dependency of the pressure drop on the media type for a structure with parallel type non-uniformity. For $0 < \xi < 1$ the parallel type non-uniform structure gives a higher pressure drop in comparison to the structure with uniform pore size distribution. For $\xi \geq 1$ the parallel type non-uniform structure gives a lower pressure drop in comparison to the structure with uniform pore size distribution.

4. Discussion

4.1. Effect of ionic strength on co-purification of contaminants

The effect of increasing ionic strength of binding buffer can sufficiently be exploited as a strategy to avoid unnecessary adsorption of low charge density impurities, such as low molecular weight RNA and proteins. Under the condition of high ionic strength of binding buffer, impurities gradually elute in the flow-through and the entire capacity of the resin can be fully utilised for pDNA adsorption. This would result in decrease in binding of undesired proteins and RNA, hence gradual diminishing of the RNA and protein peaks and increase in the pDNA concentration and purity. Also a decrease in plasmid elution time and increase in plasmid recovery with increasing ionic strength of binding buffer could be realised.

4.2. Effect of pH on pDNA binding and elution

Plasmid DNA is a large molecule and highly negatively charged. Due to its size and charge, pDNA molecules interact with a positively charged resin through several binding sites; hence the consequent interaction is very strong. The high charge density associated with pDNA molecule enables its stability under variable pH. Therefore, any change that may be observed in chromatographic performance under variable pH system almost certainly results from a change in property of the adsorbent employed. Bencina et al. [30] observed the results of pH variation employing three types of DNA: pDNA (pDNA size 5 kbp), lDNA (gDNA size 50 kbp), and gDNA with a broad molecular weight distribution up to 200 kbp. They investigated the effect of pH by changing the pH value of the mobile phase between 7 and 12. Retention of pDNA, lDNA and gDNA injected on a DEAHP (weak anion-exchanger) column significantly decreased at higher pH values. This decrease in retention was attributed to DEAHP groups since the pH variation was not expected to significantly influence the charge on the DNA. To confirm this, they conducted a similar experiment using monolithic column containing QA group, which is a strong anion-exchanger and do not change activity in the tested pH range. A comparison of DNA retention behaviour shows that the displacer concentration required for DNA elution remains similar on QA columns over the entire pH range, while there is a drastic decrease in DEAHP columns for pH values above 8, reaching no retention at pH 11.

4.3. Economics and scale up consideration of methacrylate monolith synthesis and application

On the basis of these results, the ion-exchange resin is well suited for the purification of pDNA. The binding capacity of 15.2 mg/mL obtained for the resin is higher than that of any commercially available media. The binding capacity of current commercially available adsorbents is between 0.26 and 8.86 mg/mL. However, it is the economic viability of a resin that makes it more attractive for pDNA purification especially on the commercial level. For comparison on economic grounds, the estimated cost of the DEAE-Cl functionalised resin is US$ 92 L^{-1} which is cheaper than other polymeric sorbents used for anion-exchange chromatographic purification of pDNA. The cost of functionalisation with DEAE-Cl ligand forms about 10% of the total cost as this requires energy cost to maintain a temperature of 60 °C. After several runs using the resin, it presented the same retention capacity after regeneration thus demonstrating durability and good physical resistance (Table 2). The synthesis of large-volume uniform methacrylate monolithic sorbents is a very intricate process mainly because of the large amount of exothermicity associated with the polymerisation process causing a pronounced temperature non-homogeneity that significantly affects the structure. To obtain monoliths with a reproducible and homogenous pore and surface structures, the temperature during polymerisation should be controlled. The possibilities of controlling the temperature differences inside large moulds are very limited during polymerisation and

Table 2
Binding capacity of DEAE-Cl functionalised resin with pore size 300 nm and ligand density 1.85 mmol/g measured at 1 mL/min in repeated loadings with column regeneration

Number of loadings	Binding capacity (mg/ml)
1	15.2
2	15.3
3	15.1
4	14.8
5	14.1
Resin washing and regeneration	
6	15.4
7	15.1
8	14.9
9	14.9
10	14.7

therefore the temperature gradient is determined by the experimental conditions of reactant mixture composition, the temperature of the water bath, heat transfer coefficients on either sides of the mould, the shape of the mould and the diameter of the mould. For a successful synthesis of large columns, experimental conditions have to be optimally selected with minimum exothermicity. In order to accomplish this, detailed knowledge of the kinetics of the polymer configuration and heat transfer mechanism are vital.

5. Conclusion

The unit operations of fermentation and lysis are vital stages for the production and release of pDNA from a bacterial system. However, the incorporation of monolith affects the process from the filtration stage onwards by offering fast separation at high flow rate and through-put under a reduced number of unit operations. This work utilised a methacrylate monolithic sorbent specifically tailored for direct capturing of the target pDNA molecule. Characterization of the resin showed pore and surface properties for optimum binding and retention of the pDNA molecule considering its dimension. The final product obtained after 5 min purification employing the resin was a supercoiled pDNA with no RNA or protein contamination and was found to meet regulatory standards. The sorbent displayed the potential to reduce the number of unit operations required to capture pharmaceutical grade pDNA from greater than three to one-stage purification. Scale-up and economic consideration show that this cost effective and cGMP compatible procedure can be advanced to the commercial level.

Acknowledgements

Funding for this research was kindly provided by the Victorian Endowment for Science, Knowledge and Innovation (VESKI) and via the Monash University Early Career Researcher Grant Scheme.

References

[1] M. Tyn, T. Gusek, J. Biotech. Bioeng. 35 (1990) 327.
[2] P.A. Shamlou, J. Biotechnol. Appl. Biochem. 37 (2003) 207.
[3] S. Ghose, G.M. Forde, N.K.H. Slater, J. Biotech. Prog. 20 (2003) 841.
[4] A. Jungbauer, R. Hahn, J. Sep. Sci. 27 (2004) 767.
[5] A. Strancar, A. Podgornik, M. Barut, R. Necina, in: T. Scheper (Ed.), Advances in Biochemical Engineering/Biotechnology, vol. 76, Springer, Berlin, 2002, p. 49.
[6] P. Arvidsson, F.M. Plieva, V.I. Lozinsky, I.Y. Galaev, B. Mattiasson, J. Chromatogr. A 986 (2003) 275.
[7] F.M. Kumar, I.Y. Plieva, B. Galaev, Mattiasson, J. Immunol. Meth. 283 (2003) 185.
[8] A. Mercier, H. Deleuze, O. Mondain-Monval, J. React. Funct. Polym. 46 (2000) 67.
[9] D. Josic, A. Strancar, J. Ind. Eng. Chem. Res. 38 (1999) 333.
[10] F. Svec, J.M. Fretchet, J. Ind. Eng. Chem. Res. 38 (1999) 34.
[11] H. Zou, Q. Luo, D. Zhou, J. Biochem. Biophys. Meth. 49 (2001) 199.
[12] A. Strancar, A. Podgornik, B. Milos, R. Necina, in: T. Scheper (Ed.), Advances in Biochemical Engineering/Biotechnology, 76, Springer, Berlin, 2002, p. 50.
[13] S. Xie, R.W. Allington, J.M. Fretchet, F. Svec, J. Adv. Biochem. Eng. Biotechnol. 76 (2002) 87.
[14] M. Grasselli, E. Smolko, P. Hargittai, A. Safrany, J. Nuclear. Instr. Meth. Phys. Res. Sec. 185 (2001) 254.
[15] H. Minakuchi, K. Nakanishi, N. Soga, N. Ishizuka, N. Tanaka, J. Anal. Chem. 68 (1996) 3498.
[16] N. Ishizuka, H. Minakuchi, K. Nakanishi, N. Soga, N. Tanaka, J. Chromatogr. A 797 (1998) 133.
[17] S.M. Fields, J. Anal. Chem. 68 (1996) 2709.
[18] S. Hjerten, J.L. Liao, J. Chromatogr. 457 (1988) 165.
[19] S. Hjerthen, M. Li, J. Mohammed, K. Nakazato, G. Pettersson, Nature 356 (1992) 810.
[20] B. Mayr, R. Tessadri, E. Post, M.R. Buchmeiser, J. Anal. Chem. 73 (2001) 4071.
[21] C. Liang, S. Dai, G. Guiochon, J. Anal. Chem. 75 (2003) 4904.
[22] T. Yamamoto, T. Sugimoto, T. Suzuki, S.R. Mukai, H. Tamon, Carbon 40 (2002) 1345.
[23] R. Noel, A. Sanderson, L. Spark, in: J.F. Kennedy, G.O. Philips, P.A. Williams (Eds.), A Monolithic Ion-Exchange Material Suitable for Downstream Processing of Bioproducts, in Cellulosics: Materials for Selective Separations and Other Technologies, Ellis Horwood, New York, 1993, p. 17.
[24] P.E. Gustavsson, P.O. Larsson, J. Chromatogr. A 925 (2001) 69.
[25] V.I. Lozinsky, F.M. Plieva, J. Enzyme Microb. Technol. 23 (1998) 227.
[26] E. Martin del Valle, M.A. Galan Serrano, R.L. Cerro, J. Biotechnol. Prog. 19 (2003) 921.
[27] K. Hamaker, S.L. Rau, R. Hendrickson, J. Liu, C.M. Ladisch, M.R. Ladisch, J. Ind. Eng. Chem. Res. 38 (1999) 865.
[28] N. Lendero, J. Vidic, P. Brne, A. Podgornik, A. Strancar, J. Chromatogr. A 1065 (2005) 29.
[29] J.C. Murphy, G.E. Fox, R.C. Willson, J. Chromatogr. A 984 (2003) 215.
[30] M. Bencina, A. Podgornik, A. Strancar, J. Sep. Sci. 27 (2004) 801.